

# Modelling of a phosphor plate of a white phosphor-converted remote phosphor LED

Acuña, P.<sup>1</sup>, Leyre, S.<sup>1</sup>, Audenaert, J.<sup>1</sup>, Deconinck, G.<sup>2</sup>, Meuret, Y.<sup>1</sup>, Hanselaer, P.<sup>1</sup>

<sup>1</sup>ESAT/Light & Lighting Laboratory, KU Leuven – Technology Campus, Gebroeders De Smetstraat 1, 9000 Gent, Belgium

<sup>2</sup>ESAT/ELECTA, KU Leuven, Kasteelpark Arenberg 10, bus 2445, 3001 Heverlee, Belgium  
[\\*paula.acuna@kuleuven.be](mailto:paula.acuna@kuleuven.be)

*Light extraction efficiency in SSL with conformal phosphor-converted LEDs can be enhanced with remote phosphor LED technology which allows the extraction of backscattered light and lowers the thermal operation point of the phosphor. In this study, a remote phosphor module was simulated using ray tracing software. The BRDF of the reflective material in the cavity was determined, a ray file was obtained for the blue pump LEDs, and the remote phosphor component was modeled with experimentally obtained bi-spectral BSDF data. Simulation and experimental results match in the near and far field behaviour.*

## 1. Introduction

In order to optimize a phosphor converted white LED (pcLED) system, different simulation models have been proposed for the phosphor element. In [1] and [2] a YAG phosphor is simulated within a pcLED by defining the reflected and transmitted flux of blue and yellow light measured with two integrating spheres. In [3] a model based on Mie theory using the microscopic parameters of the phosphor and the embedding matrix was defined. These models either do not consider the angular dependence in the scattering process, or they require plenty of microscopic parameters to be set in the simulation, whose acquisition is rather difficult. In [4], the interaction of the light with the phosphor is characterized by measuring the bi-directional scattering distribution function (BSDF) of a phosphor on a PET substrate and simulating the forward mode for a conformal pc LED.

A simulation model for a remote phosphor plate is proposed in this work, based on the bi-spectral BSDF, for both: backwards and forwards emission. The remote phosphor plate manufactured by Intematix consists of a diffuse polycarbonate plate coated on one side with a silicate phosphor doped with Eu. The proposed simulation model allows to analyse the influence of the incident angle on the phosphor extraction efficiency, that in turn can be used in the analysis of the recycling process due to the presence of the mixing chamber.

## 2. BSDF of the phosphor plate

The phosphor plate will be modelled based on the macroscopic scattering behaviour. The scattering of radiation can be described by the BSDF  $q_e(\theta_i, \phi_i, \theta_s, \phi_s)$ , according to [5], defined as:

$$q_e(\theta_i, \phi_i, \theta_s, \phi_s) = \frac{L_{e,\lambda,s}(\theta_i, \phi_i, \theta_s, \phi_s)}{E_{e,\lambda,i}(\theta_i, \phi_i)} \left[ \frac{1}{sr} \right] \quad \text{Eq. 1}$$

With  $L_{e,\lambda,s}(\theta_i, \phi_i, \theta_s, \phi_s)$  de radiance of the sample at a particular viewing angle  $(\theta_s, \phi_s)$ , and  $E_{e,\lambda,i}$  the irradiance on the sample from a particular incident solid angle  $(\theta_i, \phi_i)$ .

When elastic scattering occurs, i.e. there is no wavelength conversion, this expression quantifies properly the impulse response of the material to the incident light at different angles. For inelastic scattering, i.e. when wavelength conversion takes place, this

expression is not valid anymore. To extend the Nicodemus' derivation to the cross-wavelength energy transfer, the contribution of each discrete incident wavelength within the excitation range to each scattered wavelength by the fluorescent material at a certain direction  $(\theta_s, \phi_s)$  has to be considered [6]. This is called the bi-spectral BSDF, expressing the fact that scattering at one wavelength is caused by several incident wavelengths. Mathematically expressed the bi-spectral BSDF  $q_{e,\lambda}(\theta_i, \phi_i, \theta_s, \phi_s, \lambda_i, \lambda_s)$  can be defined as the derivative of the BSDF  $q_e(\theta_i, \phi_i, \theta_s, \phi_s)$  with respect to the incident wavelength  $d\lambda_i$ :

$$q_{e,\lambda}(\theta_i, \phi_i, \theta_s, \phi_s, \lambda_i, \lambda_s) = \frac{dq_e}{d\lambda_i} = \frac{dL_{e,\lambda,s}(\theta_i, \phi_i, \theta_s, \phi_s, \lambda_s)}{E_{e,\lambda,i}(\theta_i, \phi_i, \lambda_i) \cdot d\lambda_i} \left[ \frac{1}{sr \cdot nm} \right] \quad \text{Eq. 2}$$

In order to know the contribution of an incident wavelength range  $\Lambda_i$  to the spectral scattered flux at the scattered wavelength  $\lambda_s$ , it is necessary to integrate Eq. 2 with respect to  $d\lambda_i$  over a particular range. The integration range is between 450 and 470 nm for incident blue light, mimicking the emission of blue LEDs. From this result an average value  $\langle q_{e,\Lambda_i} \rangle$  can be calculated for any scattered wavelength  $\lambda_s$  as a function of the scattered angle  $(\theta_s)$

$$\langle q_{e,\Lambda_i}(\theta_i, \phi_i, \theta_s, \phi_s, \lambda_s) \rangle = \frac{L_{e,\lambda,s}(\theta_i, \phi_i, \theta_s, \phi_s, \lambda_s)}{\int_{\lambda_i=450}^{\lambda_i=470} E_{e,\lambda,i}(\theta_i, \phi_i, \lambda_i) \cdot d\lambda_i} \left[ \frac{1}{sr \cdot nm} \right] \quad \text{Eq. 3}$$

Simulation of the detailed bi-spectral BSDF is extremely cumbersome, therefore it is simplified by simulating only two wavelengths, yet properly reproducing the conversion and scattering behaviour of the phosphor plate. Each wavelength takes an average value resulting from the integration of  $\langle q_{e,\Lambda_i} \rangle$  over the scattered wavelengths, for both the BRDF and the BTDF.

### 3. Experiments and Simulation

This plate is meant to be excited by pump-LEDs whose emission peak is about 450 nm, resulting in white light with a CCT of 3000 K. The BSDF for the phosphor plate was characterized with the setup described in [7], consisting of a goniometer with a fixed position light source and a mobile detector, with a position and inclination adjustable sample holder in between the light source and the detector. For every incident polar angle  $(\theta_i = 5^\circ, 45^\circ, 56^\circ)$  the scattered spectral flux  $\Phi_{e,\lambda,s}$  was measured for the scattered polar angles  $0^\circ \leq \theta_s \leq 90^\circ$  in the incident plane in increments of  $5^\circ$  for both the reflection (backwards) and transmission (forwards) hemispheres. Two incident spectra have been applied: "blue light" within the excitation spectrum (Figure 1-right) of the fluorescent material mimicking the pump-LED and "yellow light". The BSDF measurement when "yellow light" impinges is required in order to characterize the interaction between the phosphor plate and the emission spectrum of the phosphor after being reflected in the mixing cavity.

In total three different BSDFs are defined, corresponding to the elastic and inelastic scattering in response to the blue incident light, and to the elastic scattering in response to the yellow incident light. These functions are converted into tables that define the scattering simulation model in the ray tracing program. Each of this functions are assigned as a surface property to the geometrical representation of the phosphor plate. The mixing chamber consists of a cylindrical cavity with radius 35 mm and height 43 mm, whose inner surface has the BRDF characteristic of an MPET material. The light

source is represented by a ray-file of four blue LEDs located at the base of the mixing chamber and equidistantly distributed along a radius of 18 mm (Figure 1 -left). The ray-file was measured by a near-field goniometer equipped with a luminance camera (TechnoTeam Rigo 801).

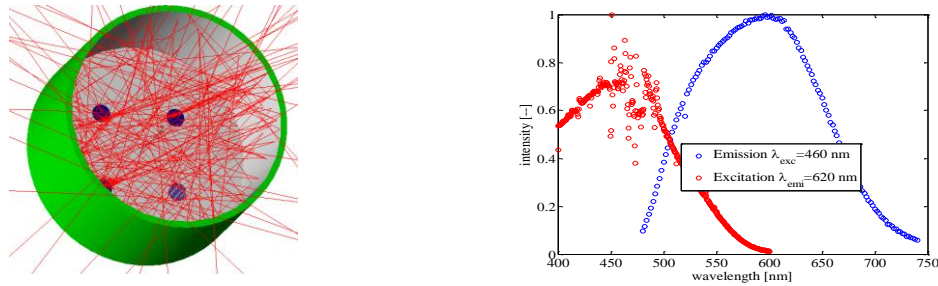


Figure 1 Whole module simulation in ray tracing (left); Excitation and emission spectrum for the phosphor plate (right)

#### 4. Results and Discussion

From the phosphor characterization one incident angle is chosen ( $\theta_i = 45^\circ$ ) to illustrate the response of the phosphor plate to the blue and yellow light.

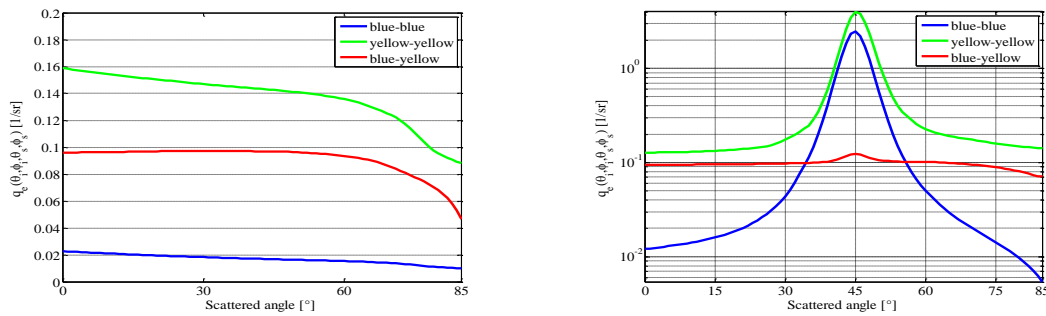
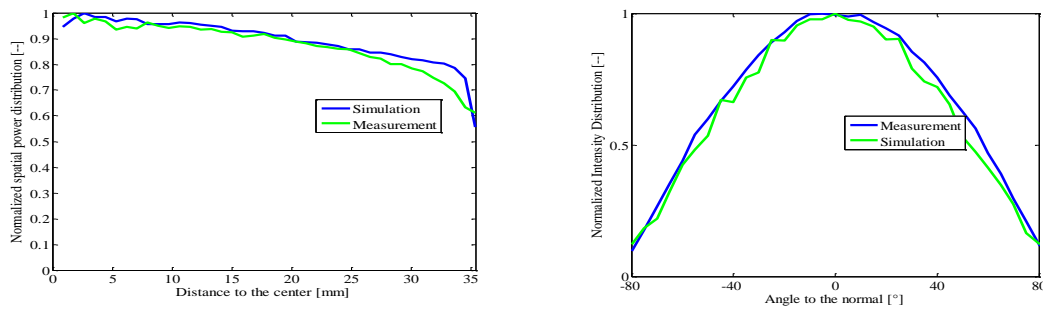


Figure 2 Responses of the phosphor plate to excitation at an incident angle of  $45^\circ$ . Bi-directional transmittance distribution function (Left); Bi-directional reflectance distribution function (Right)

From Figure 2 the transmittance distribution function presents a rather lambertian behaviour for the three responses due to the effect of the diffuse (polycarbonate) plate along with the phosphor coating. On the other hand, the reflectance distribution functions present higher values around the specular angle for the elastic scattering, and lambertian for the inelastic scattering.

To validate the simulation model of the whole module it has been compared: (1) the spatial distribution of the exitance at the outer surface of the phosphor plate, and (2) the intensity distribution in the far-field region. The spatial distribution of the exitance was calculated for each concentric ring equally distributed over the phosphor plate.

A good agreement exists between the experimental and simulation results as showed in Figure 3. From the simulation it is possible to determine the increment in light extraction due to the light recycled by the mixing chamber. Simulations performed when attributing a reflectance of zero to the mixing chamber are compared to the simulation results when the MPET characteristics have been used. The light extraction with the mixing chamber is 1.7 times the amount of light extracted when the mixing chamber is totally absorbing. These results are confirmed with integrating sphere spectral radiant flux measurements of the whole module, equipped with reflecting and absorbing walls of the mixing chamber respectively.



**Figure 3** Validation of the simulation model for the whole module. The exitance over concentric rings characterized by the distance to the centre (left) and the normalized intensity distribution (right).

## 5. Conclusions

The simulation model of a cylindrical mixing chamber covered by a remote phosphor plate (a phosphor coating in combination with a diffuse polycarbonate plate) has been developed. This model allows to predict the response of the phosphor plate to different mixing chamber designs. Future work will be focused towards the use of the model in optimizing the geometry and form factor of the mixing chamber.

### Acknowledgments

The authors appreciate the financial support of: the Hercules Foundation – project AKUL035 “Near-Field Imaging Luminance Goniometer”, Colciencias (Administrative Department of Science, Technology and Innovation - Colombia) (Paula Acuña), and the Agency for Innovation by Science and Technology in Flanders (IWT) (SB-091442, Jan Audenaert). The authors wish to thank Professor. Philippe Smet for his help in conducting the fluorescence measurements of the phosphor plate.

### References

- [1] K. Yamada, Y. Imai, and K. Ishii, "Optical Simulation of Light Source Devices Composed of Blue LEDs and YAG Phosphor," *Journal of Light & Visual Environment*, vol. 27, p. 70, 2003.
- [2] Y. Zhu and N. Narendran, "Investigation of Remote-Phosphor White Light-Emitting Diodes with Multi-Phosphor Layers," *Japanese Journal of Applied Physics*, vol. 49, no. 10, p. 100203, Oct 2010.
- [3] Christian Sommer, Paul Hartmann, Peter Pachler, Hans Hoschopf, and Franz P. Wenzl, "
- [4] Chien-Hsiang Hung and Chung-Hao Tien, "Phosphor-converted LED modeling by bidirectional photometric data," *Opt. Express*, vol. 18, no. S3, pp. A261--A271, Sep 2010. [Online]. <http://www.opticsexpress.org/abstract.cfm?URI=oe-18-103-A261>
- [5] F. E. Nicodemus, *Geometrical considerations and nomenclature for reflectance*, U.S. Government Printing, Ed.: U.S. Dept. of Commerce, National Bureau of Standards : for sale by the Supt. of Docs., U.S. Govt. Print. Off. (Washington), October 1977.
- [6] Matthias B. Hullin et al., "Acquisition and analysis of bispectral bidirectional reflectance and reradiation distribution functions," *ACM Trans. Graph.*, vol. 29, no. 4, pp. 97:1--97:7, #jul# 2010. [Online]. <http://doi.acm.org/10.1145/1778765.1778834>
- [7] Frederic B. Leloup, Stefaan Forment, Philip Dutré, Michael R. Pointer, and Peter Hanselaer, "Design of an instrument for measuring the spectral bidirectional scatter distribution function," *Appl. Opt.*, vol. 47, no. 29, pp. 5454-5467, Oct 2008. [Online]. <http://ao.osa.org/abstract.cfm?URI=ao-47-29-5454>
- [8] ASTM Standard E1392, 1996(2002), Standard Practice for Angle Resolved Optical Scatter Measurements on Specular or Diffuse Surfaces, 2002.